Bone marrow-derived mesenchymal cells and MMP13 contribute to experimental choroidal neovascularization

Julie Lecomte[1§], Krystel Louis[1§], Benoit Detry[1], Silvia Blacher[1], Vincent Lambert[1,2], Sandrine Bekaert[1], Carine Munaut[1], Jenny Paupert[1], Pierre Blaise[2], Jean-Michel Foidart[1], Jean-Marie Rakic[2], Stephen M. Krane[3], Agnès Noel[1*].

[§]These authors contributed equally.

[1]Laboratory of Tumor and Developmental Biology, Groupe Interdisciplinaire de Génoprotéomique Appliquée-Research (GIGA-Cancer), University of Liege, Tour de Pathologie (B23), B-4000 Liège, Belgium; [2]Department of Ophthalmology, CHU, B-4000 Liège, [3]Center for Immunology and Inflammatory Disease, Department of Medicine, Harvard Medical School and Massachusetts General Hospital, Building 149, 13th Street, Room 8301, Boston, MA 02129.

*Editorial correspondence: A. NOEL
Laboratory of Tumor and Developmental Biology
University of Liège, Tour de pathologie, CHU (B23)
Sart-Tilman, B-4000 Liège, Belgium
Tel: 32-4-366.25.69, Fax: 32-4-366.29.36
e-mail: agnes.noel@ulg.ac.be

Running title : MMP13 in choroidal neovascularization.

ABSTRACT

In this study, we evaluate the potential involvement of collagenase-3 (MMP13), a matrix metalloproteinase (MMP) family member, in the exudative form of age-related macular degeneration (AMD) characterized by a neovascularisation into the choroid. RT-PCR analysis revealed that human neovascular membranes issued from patients with DMLA expressed high levels of *Mmp13*. The contribution of MMP13 in choroidal neovascularization (CNV) formation was explored by using a murine model of laser-induced CNV and applying it to wild type mice (*WT*) and *Mmp13*-deficient mice ($Mmp13^{-/-}$ mice). Angiogenic and inflammatory reactions were explored by immunohistochemistry. The implication of bone marrow (BM)-derived cells was determined by BM engraftment into irradiated mice and by injecting mesenchymal stem cells (MSC) isolated from WT BM. The deficiency of Mmp13 impaired CNV formation which was fully restored by WT BM engraftment and partially rescued by several injections of WT MSC. The present study sheds light on a novel function of MMP13 during BM-dependent choroidal vascularization and provides evidence for a role for MSC in the pathogenesis of CNV.

Keywords: CNV, MMP13, angiogenesis, bone marrow, mesenchymal stem cells.

Non-standard abbreviations used:

AMD: age-related macular degeneration; BM: bone marrow ; CAM: choroiallantoic membrane ; CNV: choroidal neovascularisation ; MSC: mesenchymal stem cells ; RPE: retinal pigmented epithelium ; TIMP: tissue inhibitor of metalloprotease.

INTRODUCTION

Age-related macular degeneration (AMD) is one of the most common irreversible causes of blindness among people over 50 years [1]. Ninety percents of all vision loss due to AMD occurs in the exudative form which is characterized by choroidal neovascularization (CNV). The newly formed blood vessels arising from choriocapillaries are directed to the subretinal macular region with subsequent bleeding and/or fluid leakage into the subretinal space, local retinal detachment and retinal photoreceptor damage [2]. The pathophysiology of AMD is complex and age-related changes that induce pathologic neovascularization are incompletely understood. In combination with the rapidly growing knowledge on basic mechanisms in angiogenesis, new evidence in pathogenesis of macular disease have led to novel developments in therapeutic strategies. Indeed, angiogenic factors such as VEGF play an important role in choroidal neovascular formation [3-5] and anti-VEGF molecules represent a substantial tool against AMD [6]. In the process of CNV, the vascular overgrowth is coupled with a localized proteolysis, extracellular remodelling and cell migration involving different proteolytic systems among which the matrix metalloproteinases (MMPs) are key players [7-9].

An involvement of MMPs in the progression of retinal and choroidal neovascularization is supported by both experimental and clinical data. A mutation of *Timp-3* gene (tissue inhibitor of metalloproteinase-3) is the cause of a rare familial form of macular dystrophy associated with subretinal neovascularisation [10-12]. We previously reported the contribution of different MMPs, such as MMP2 or MMP9, in a mouse model of choroidal neovascularisation [13]. Here, we focused our interest on MMP13, an important collagenase displaying distinct properties compared with the other collagenases: MMP1 (interstitial collagenase), MMP8 (neutrophil collagenase) and MMP14 (MT1-MMP) [14]. MMP13 has the capacity to cleave native fibrillar collagen types I, II, III, and V as well as several other extracellular matrix (ECM) components, including type IV, X, and XIV collagens, large tenascin C, fibronectin, aggrecan, versican and fibrillin [15-19]. A role for MMP13 in cartilage matrix degradation has been proposed based on its expression during endochondral ossification and its particular potential to degrade type II collagen [20;21]. An involvement of MMP13 in angiogenesis has been documented in the chorioallantoic membrane (CAM) of the chick embryos [22], in bone fracture healing [23] and in the maintenance of the angiogenic response induced in developing skin carcinomas [24]. Nevertheless, a possible involvement of MMP13 in the neo-vascularization associated with ocular diseases has not been examined.

In the current study, we provide evidence for MMP13 expression in late stages of human exudative AMD and investigate the potential role of MMP13 in choroidal angiogenesis in a murine model of laser-induced ocular neovascularisation. We demonstrate the contribution of MMP13 in experimental CNV and a MSC-mediated modulation of this angiogenic process.

MATERIAL AND METHODS

Mice

Homozygous *Mmp13*-deficient mice (*Mmp13*$^{-/-}$) and the corresponding wild-type mice (*WT*) were generated in C57BL/6 background as previously described [25]. Mice expressing a single copy of a transgene that encodes the enhanced green fluorescent protein (eGFP) under the control of ß-actin promoter C57BL/6-Tg(ACTbEGFP)10sb were obtained from the Jackson Laboratories (Bar Harbor, ME). Experimental procedures were performed in accordance to the guidelines of the University of Liège regarding the care and use of laboratory animals and are in line with the "Ethical principles and guidelines for scientific experiments on animals" of the Swiss Academy of Medical Sciences.

BM Transplantation

BM cells were isolated from the tibia and femur of donor mice (8 to 10 weeks of age) by slowly flushing DMEM culture medium (Gibco BRL, Paisley, UK) into the diaphyseal channel. Recipient mice (8 to 10 weeks old) sublethally irradiated with a single dose of 9 Gy were injected intravenously (i.v.) with BM cells (10^7 per animal). At 5 weeks after BM transplantation, impact laser burns were performed. The success of BM transplantation was assessed as previously described [26].

CNV Model

CNV was induced in both eyes of mice by photocoagulation with laser burns as previously described [27]. After 14 days (or earlier time points in kinetic analysis), animals were sacrificed and both eyes were enucleated (n = 4 to 8 animals per experimental condition with 4 lesions per eye). For immunohistochemical analysis, eyes were embedded in Tissue Tek for cryostat sectioning. Neovascularization was estimated by computer-assisted measurement on at least five sections per lesion of the b/c ratio (b, thickness from the bottom of the pigmented choroidal layer to the top of the neovascular membrane; c, thickness of the intact pigmented choroid adjacent to the lesion) as previously described [28-30].

For confocal visualization of the vasculature, mice were injected intravenously with 200 µl of fluorescein isothiocyanate (FITC)-conjugated dextran (2×10^3 kd average molecular weight, Sigma) (50 mg/ml). After 1 hour of fixation in paraformaldehyde 1% (pH 7.4), retinas were removed and choroids were flat-mounted using Vectashield mounting medium (Vector Laboratories, Burlingame, CA). Spatial distribution of fluorescence was examined using a Leica TCS SP2 inverted confocal laser microscope (Leica Microsystems, Wetzlar, Germany) equipped with one argon and two helium-neon lasers and an acousto-optical tuneable filter for excitation intensity. FITC was visualized by using an excitation wavelength of 488 nm, and the emission light was dispersed and recorded from 500 to 535 nm. For each lesion, serial optical sections were recorded with a z-step of 1.67 µm. After successive scanning for each interval, three-dimensional fluorescent images were constructed by using Leica confocal software. The area and the volume of CNV on choroidal flatmount were determined using the image analysis toolbox of MATLAB 7.9 software.

Human neovascular membranes

Submacular CNV specimens were obtained during surgery for 360° macular translocation performed on patients (n =3) with exudative AMD, either not amenable to conventional laser/photodynamic therapy (presence of occult new vessels or submacular bleeding) or in one patient, due to a severe recurrence a few months after a successful medical treatment [31]. The neovascular membranes were snap frozen in liquid nitrogen and stored at -80°C. Intact posterior segments from healthy donors (Cornea Bank, Liège, Belgium) collected maximum 8 hours after death were used as controls (n = 4). GAPDH was used as a control to check for RNA degradation. The methods conformed to the Declaration of Helsinki for research involving human subjects.

RNA extraction in experimental CNV

To evaluate the kinetics of MMP expression, choroidal neovascularization was induced in mice by multiple argon laser burns and animals were killed at days 3, 5, 10, 14, 20, and 40. The posterior segments (RPE-choroid complex without neural retina) were cut out and immediately frozen in liquid nitrogen. Total RNA was extracted (RNeasy extraction kit, Quiagen, Paris, France) according to the protocol of the manufacturer.

In some assays, choroidal neovascular membranes and adjacent neural retina intact regions were separately extracted from frozen sections by laser capture microdissection (laser pressure catapulting [LPC] technique) as previously described [32]. Total RNA isolation was performed (TRIzol Reagent, Life Technologies, Carlsbad, California, USA) according to the manufacturer's protocol.

RT-PCR analysis

RT-PCR was done on 10 ng of total RNA extracted from tissue using a GeneAmp Thermostable rTth Reverse Transcriptase RNA PCR kit (Applied Biosystems, Foster City, CA) following manufacturer's instructions. Specific pairs of primers (Eurogentec, Seraing, Belgium) for mouse *Mmp13* were designed as follows: forward (Exon 6), ATGATCTTTAAAGACAGATTCTTCTGC-3'; reverse (Exon 7), 5'-TGGGATAACCTTCCAGAATGTCATAA-3'. Amplification of 35 cycles was run for 15 seconds at 94°C, 20 seconds at 68°C, and 30 seconds at 72°C. Quantification of Mmp13 expression quantification was normalized to 28S signal. Note that the mutation in $Mmp13^{-/-}$ mice is in Exon 5 that encodes the critical catalytic domain of the enzyme. This exon is spliced out in the $Mmp13^{-/-}$ mice [33].

Immunohistochemistry

Cryostat sections (6 μm in thickness) were fixed in acetone at –20°C and in methanol 80% at 4°C before incubation with primary antibodies (Abs). For double-immunofluorescent-labelling, sections were incubated with two primary Abs. Abs raised against MMP13 (sheep y anti mouse, diluted 1/200; home-made Ab from Dr. M.Muller, Heidelberg, Germany), PECAM/CD31 (rat anti-mouse, diluted 1/100; BMA, Switzerland), NG2 chondroitin sulfate proteoglycan (pericytes, rabbit anti-rat, diluted 1/200; Chemicon, Temecula, CA), α-smooth muscle actin (FITC-coupled mouse monoclonal, diluted 1/200; Sigma-Aldrich), neutrophils (rat anti-mouse, diluted 1/20; Serotec, Oxford, UK), CD11b (biotin-coupled rat anti-mouse, diluted 1/250; Pharmingen, San Diego, CA) were incubated for 1 hour at room temperature. After washings, the appropriate secondary Abs conjugated to FITC, TRITC or Texas Red were applied for 30 minutes, rabbit anti-sheep (dilution 1/500; Cappel Pharmaceuticals), swine anti-rabbit (diluted 1/40; Dakopat, Glostrup, Denmark), mouse anti-guinea pig (diluted 1/40; Sigma), and goat anti-rat (diluted 1/100; Molecular Probes, Eugene, OR). For the CD11b labelling, CY3 conjugated streptavidin (diluted 1/200, Sigma) was applied after washing the sections. For measurement of vessel coverage with pericytes, automatic computer-assisted image analysis was performed in image of lesions obtained after double immunostaining for CD31 and NG2. The ratio between the surface of CD31 staining and NG2 staining was measured by using Aphelio 3.2 software (Asis, France) [34].

Isolation and expansion of murine Mesenchymal Stem Cell (MSC)

MSC were obtained from at least 2 C57Bl/6J mice 8 to 10 weeks old. BM cells were isolated from the tibia and femur of donor mice as described above for BM transplantation. BM cells were filtrated and plated in Mesencult medium (StemCell Technologies Inc, Vancouver, Canada). After 24h, nonadherent cells were removed by washing with phosphate-buffered saline (PBS) and fresh medium was added. MSC were used from passages 6 to 10. MSC phenotype was characterised by immunostaining and FACS analysis ($CD106^{+}$, $Sca1^{+}$, $CD34^{-}$, $CD45^{-}$, $CD11b^{-}$). Osteogenic, adipogenic and chondrogenic differentiation assays were performed on MSC as previously described [35].

Statistical analyses

Data were analyzed with GraphPad Prism 4.0 (San Diego, CA). The unpaired Student's t test was used to determine the significance ($p<0.05$) of differences between experimental groups ($*$: $p<0.05$; $**$: $p<0.01$; $***$: $p<0.001$).

RESULTS

Mmp13 is expressed in human neovascular membranes and in mouse choroidal neovascular lesions induced by laser burn

Mmp13 mRNAs expression was evaluated on submacular CNV specimens collected on AMD patients during surgery for 360° macular translocation. *Mmp13* mRNAs were strongly expressed in all human CNV specimens analysed (Figure 1A). In sharp contrast, a faint basal expression of *Mmp13* mRNA was detected in some control specimens (in or out of the macula) collected from healthy donors. The expression of *28S* rRNA and *Gapdh* mRNA was used as a control to assess the good preservation of mRNA in AMD patients and healthy donors.

In mouse, photocoagulation with an argon laser induced a trauma leading to the formation of choroidal neovascular lesions (CNV) under the retina. RT-PCR analysis revealed that levels of *Mmp13* mRNA were low in the early stage of CNV formation and then progressively increased from day 5 to day 7 ($p< 0.05$). From day 7 to day 14, coinciding with the period of CNV stabilization, *Mmp13* mRNA levels did not progress anymore ($p= 0.3627$) ($n=8$) (Fig.1A). *Mmp13* mRNAs were specifically detected on microdissected neovascular choroidal membranes from *WT* mice, but not from *Mmp13*$^{-/-}$ mice. Neighbouring intact chorioretinal areas were negative for *Mmp13* mRNA, confirming that *Mmp13* expression was locally induced during the photocoagulation (Fig.1B). Immunohistochemical analysis confirmed the presence of MMP13 protein in the neovascular lesions in *WT* mice (Fig.3A, B).

Mmp13-deficiency impairs choroidal neovascularization

Retinal damage and choroidal neovascularization were estimated by measuring different parameters: the area of CNV on choroidal flatmounts observed by confocal microscopy (Fig.2A) and the ratio between the maximal height of the lesion (b) and the thickness od the normal choroid (c) observed in the neighbouring intact zones (b/c ratio) determined on tissue sections (Fig.2B) [36]. A reduced neovascularization was observed in *Mmp13*$^{-/-}$ mice as compared to *WT* mice. The analysis by confocal microscopy of flatmounted choroids revealed a two-fold reduction of vessel area (Fig.2A). Similar results were obtained by measuring the volume of vascularisation through a 3D analysis ($0.11x10^6$ $\mu m^3 \pm 0.03x10^6$ SEM in *WT* mice versus $0.05x10^6$ $\mu m^3 \pm 0.01x10^6$ SEM in *Mmp13*$^{-/-}$ mice; $p=0.047$). The severity of neovascularisation was also estimated histologically on serial sections by measuring the maximal height of lesion (b) above the thickness of the normal choroid observed in neighbouring intact zones (c). In *Mmp13*$^{-/-}$ mice, the b/c ratio was significantly reduced in comparison to *WT* mice ($P < 0.0001$) (Fig.2B). Newly formed blood vessels were characterized by immunostaining of endothelial cells (PECAM positive cells) and perivascular cells (αSMA positive cells) or pericytes (NG2 positive cells) (fig.3C-F). While newly formed vessels were "naked" in *Mmp13*$^{-/-}$ mice, they were covered by $NG2^+$ cells and αSMA^+ cells in *WT* mice. Indeed, the percentage of NG2/SMA co-localization was 10-fold higher in *WT* mice as compared to *Mmp13*$^{-/-}$ mice (9.18 ± 3.45 in WT *versus* 0.97 ± 0.39 in KO mice). These results reveal that *Mmp13* deficiency not only affected vessel recruitment, but also impaired their maturation through pericyte coverage.

The inflammatory reaction was next explored by immunostaining of CD11b (Fig.3G,H) and neutrophils (Fig.3I,J). In accordance with our previous data [37], inflammatory cells were not detected before injury induction (at day 0) and appeared at day 3 post-injury. No significant difference in the number of inflammatory $CD11b^+$ cells was observed in *Mmp13*-deficient mice (0.077 ± 0.006 $CD11b^+$ cells per mm^2 and 0.064 ± 0.005

cells neutrophils per mm²) compared to the *WT* mice (0.051 ± 0.003 cells $CD11b^+$ cells per mm² and 0.048 ± 0.009 cells neutrophils per mm²) ($p>0.05$).

WT bone marrow-derived cells rescue choroidal angiogenesis in *Mmp13*-deficient mice

BM was harvested from *WT* mice and RT-PCR analysis revealed *Mmp13* expression in BM cells. *WT* or *Mmp13*$^{-/-}$ mice were irradiated and transplanted with unfractionned BM issued from *WT* or *Mmp13*$^{-/-}$ mice. Five weeks after BM transplantation (i.e., after allowing for BM reconstitution), laser burns were performed to induce CNV. Genotyping of spleen was performed for all animals to assess BM transplantation success. New blood vessel formation was quantified by both flatmount and histological analysis. When irradiated mice were reconstituted with BM from *WT* mice, a slight decrease but not significant ($P>0.05$) in vessel formation was observed in grafted mice as compared to ungrafted mice (Fig.4). Interestingly, a complete restoration of the CNV was observed in *Mmp13*$^{-/-}$ mice engrafted with *WT* BM. In this experimental group, the CNV formation was similar to that observed in *WT* mice engrafted with *WT* BM and significantly higher than that of *Mmp13*$^{-/-}$ mice engrafted with *Mmp13*$^{-/-}$ BM ($p=0.0097$). Moreover, the engraftment of *MMP13*-deficient BM into *WT* mice significantly decreased CNV formation in comparison to *WT* control mice ($p=0.0009$) (Fig.4). Similar results were obtained by evaluating CNV formation through confocal analysis of flatmount choroids (fig.4A) and through histological analysis of eye sections (fig.4B).

Bone marrow-derived MSC are implicated in *Mmp13*-mediated choroidal angiogenesis

Effects of BM-produced MMP13 could be either attributed to hematopoietic cells but also to mesenchymal stem cells (MSC). It has been described that MMP13 is mainly expressed by mesenchymal cells [38]. To provide new insights into the type of BM-derived cells involved in CNV formation, we isolated (MSC) from *WT* BM. The expression of *Mmp13* by MSC cultured cells was assessed by RT-PCR analysis. *Mmp13* mRNA is more expressed by isolated MSC than by whole bone marrow (Fig.5B). MSC were then intravenously injected at days 1, 3, 7 and 10 post laser injury. Interestingly, MSC injection into *WT* mice did not affect CNV formation (Fig.5A). In contrast, a partial restoration of CNV formation was observed in *Mmp13*-deficient mice injected with *WT* MSC. These results demonstrate a contribution of MSC in CNV formation mediated by MMP13.

DISCUSSION

Through a genetic approach, the present study provides evidences for a contribution of MMP13 during BM-dependent choroidal neovascularization in a mouse model of laser burn-induced CNV. This concept is supported by [1] the increased expression of *Mmp13* during the course of CNV induction, [2] the impaired CNV in *Mmp13*$^{-/-}$ mice and [3] the restoration of CNV in *Mmp13*$^{-/-}$ mice by the engraftment of BM or the injection of MSC derived from *WT* mice. These experimental findings are consistent with the expression of MMP13 detected in late stages of human exudative AMD.

The contribution of MMP13 in angiogenesis has been previously documented in a physiological model of angiogenesis, the chorioallantoic membrane (CAM) assay [39]. In this system, purified chicken MMP13 elicited an angiogenic response in the CAM onplant comparable to that induced by angiogenic growth factors. In line with our finding of angiogenesis dysfunction in *Mmp13*-deficient mice, is the observation of defective vascular penetration into the fracture callus observed in a murine model of bone fracture healing [40], impaired tumoral angiogenesis in murine models of skin carcinomas [41] and delayed vascularization of primary ossification centres in *Mmp13*$^{-/-}$ mice during embryonic development [42]. Our work extends the role of MMP13 to pathological angiogenesis and specifically to ocular diseases such as AMD.

The action of MMP13 in CNV can involve different mechanisms. As a principal interstitial collagenase, MMP13 could contribute to tissue remodelling paving the way for endothelial cell migration. We found, however, that collagen deposition assessed by safranin staining did not reveal differences between genotypes (data not shown). MMP13 could also participate in a proteolysis cascade including MT1-MMP, MMP2 and MMP9 [43]. Indeed, the latter MMPs could have the most critical function in extracellular matrix remodelling occurring during angiogenesis associated with AMD. In this context, we previously reported the key contribution of MMP2 and MMP9 in CNV [44]. A pro-angiogenic effect of MMP13 may also require release from cryptic sites of angiogenic factors such as bFGF [45] or VEGF [46]. A combination of different mechanisms of action cannot be excluded. The present demonstration that MMP13 plays a role in CNV provides an incentive to further study the mechanisms underlying the pro-angiogenic functions of MMP13.

An unexpected finding of our work is the contribution of BM-derived cells to the pro-angiogenic action of MMP13. The formation of choroidal neovascularization may involve different mechanisms such as angiogenesis (the endothelial cell spouting from pre-existing vessels) and vasculogenesis (the recruitment of BM-derived cells) [47-49]. We and others previously demonstrated the recruitment of BM-derived cells in CNV [50-54]. These observations are further supported by previous experiments in which GFP^{+} BM cells were engrafted into *WT* mice [54-58]. Of interest is the demonstration here that *WT* BM-derived cells are sufficient to restore the vascularization impaired by *Mmp13* deficiency. This report provides the first experimental evidence for a key role played by BM-derived MMP13 in pathological ocular vascularization. This is in line with the levels of MMP13 expression reported in BM-derived cells that contributed to the pathology in a model of liver fibrosis [59]. It is worth noting that whole body irradiation followed by bone marrow reconstitution can potentially affect neovascularization. Indeed, radiation is well known to cause damage to endothelial cells and to inhibit neovascularization by suppressing the recruitment of bone marrow-derived endothelial cells [60]. Accordingly, a slight radiation-induced defect in neovascularization was observed in the present model. The present study demonstrates that *Mmp13*$^{-/-}$ mice engrafted with *WT* BM displayed similar CNV formation than *WT* mice engrafted with WT BM revealing a restoration of the angiogenic response through BM transplantation.

The effect of BM-derived cells could be attributed to MSC, vascular progenitor cells and/or inflammatory cells which could migrate into reconstituted tissues or secrete soluble factors that mediate inflammation and angiogenesis. We previously demonstrated that several BM-derived cells could contribute to CNV development, such as inflammatory CD11b positive cells and/or mesenchymal cells positive for αSMA (myofibroblasts or vascular smooth muscle cells) [61]. In the current study, we demonstrate the key role in CNV formation played by Mmp13-expressing MSC. Indeed, four repetitive injections of MSC derived from *WT* mice partially rescued the impaired

angiogenic phenotype in *Mmp13*$^{-/-}$ mice. This partial restoration achieved with MSC injection as compared to the complete restoration of the phenotype achieved with BM engraftment could be explained either by a combined effect of different types of BM-derived cells, a transient effect of MSC or an insufficient supplementation of MSC through cell injections. Nevertheless, these data point to a novel role for MSC in CNV.

In conclusion, we have identified MMP13 as a key regulator of choroidal angiogenesis. Our findings extend the potential roles of MMP13 initially observed in cartilage/bone resorption [62] and tumor development [63;64] to ocular diseases such as AMD. This pro-angiogenic effect of MMP13 is mainly mediated by BM-derived mesenchymal cells. These findings pave the way for therapeutic strategies based on the targeting of MMP13 with synthetic inhibitors or on the use of MSC as delivery vehicle for anti-angiogenic agents as a "Trojan horse" approach [65].

ACKNOWLEDGMENTS

The authors acknowledge P. Gavitelli, F. Olivier, M.-R. Pignon, E. Feiyereisen, L. Poma, G. Roland and N. Lefin for collaboration and technical assistance. They thank the GIGA imaging and flow cytometry platform for their help. This work was supported by grants from the European Union Framework Program projects (FP7, MICROENVIMET), the Fonds de la Recherche Scientifique Médicale, the Fonds National de la Recherche Scientifique (F.N.R.S., Belgium), the Federation belge contre le Cancer, the Fonds spéciaux de la Recherche (University of Liège), the Centre Anticancéreux près l'Université de Liège, the Fonds Léon Fredericq (University of Liège), the D.G.T.R.E. from the « Région Wallonne », the Interuniversity Attraction Poles Program - Belgian Science Policy (Brussels, Belgium). JL is recipient of a Televie-FNRS grant. SMK was supported by a grant from the US National Institutes of Health.

Reference List

1. Bressler NM (2004) Age-related macular degeneration is the leading cause of blindness.. JAMA, 291: 1900-1901.
2. Rattner A, Nathans J (2006) Macular degeneration: recent advances and therapeutic opportunities. Nat. Rev. Neurosci., 7: 860-872.
3. Ferrara N, Kerbel RS (2005) Angiogenesis as a therapeutic target. Nature, 438: 967-974.
4. Noel A, Jost M, Lambert V, Lecomte J, Rakic JM (2007) Anti-angiogenic therapy of exudative age-related macular degeneration: current progress and emerging concepts. Trends Mol. Med., 13: 345-352.
5. Rakic JM, Lambert V, Devy L, Luttun A, Carmeliet P, Claes C, Nguyen L, Foidart JM, Noel A, Munaut C (2003) Placental growth factor, a member of the VEGF family, contributes to the development of choroidal neovascularization. Invest Ophthalmol. Vis. Sci., 44: 3186-3193.
6. Noel A, Jost M, Lambert V, Lecomte J, Rakic JM (2007) Anti-angiogenic therapy of exudative age-related macular degeneration: current progress and emerging concepts. Trends Mol. Med., 13: 345-352.
7. Rundhaug JE (2005) Matrix metalloproteinases and angiogenesis. J. Cell Mol. Med., 9: 267-285.
8. Raffetto JD, Khalil RA (2008) Matrix metalloproteinases and their inhibitors in vascular remodeling and vascular disease. Biochem. Pharmacol., 75: 346-359.
9. Noel A, Jost M, Lambert V, Lecomte J, Rakic JM (2007) Anti-angiogenic therapy of exudative age-related macular degeneration: current progress and emerging concepts. Trends Mol. Med., 13: 345-352.

10. Das A, McGuire PG, Eriqat C, Ober RR, DeJuan E Jr, Williams GA, McLamore A, Biswas J, Johnson DW (1999) Human diabetic neovascular membranes contain high levels of urokinase and metalloproteinase enzymes. Invest Ophthalmol. Vis. Sci., 40: 809-813.
11. Kadonosono K, Yazama F, Itoh N, Sawada H, Ohno S (1999) Expression of matrix metalloproteinase-7 in choroidal neovascular membranes in age-related macular degeneration. Am. J. Ophthalmol., 128: 382-384.
12. Weber BH, Vogt G, Pruett RC, Stohr H, Felbor U (1994) Mutations in the tissue inhibitor of metalloproteinases-3 (TIMP3) in patients with Sorsby's fundus dystrophy. Nat. Genet., 8: 352-356.
13. Lambert V, Wielockx B, Munaut C, Galopin C, Jost M, Itoh T, Werb Z, Baker A, Libert C, Krell HW, Foidart JM, Noel A, Rakic JM (2003) MMP-2 and MMP-9 synergize in promoting choroidal neovascularization. FASEB J., 17: 2290-2292.
14. Overall CM, Lopez-Otin C (2002) Strategies for MMP inhibition in cancer: innovations for the post-trial era. Nat. Rev. Cancer, 2: 657-672.
15. Fosang AJ, Last K, Knauper V, Murphy G, Neame PJ (1996) Degradation of cartilage aggrecan by collagenase-3 (MMP-13). FEBS Lett., 380: 17-20.
16. Knauper V, Smith B, Lopez-Otin C, Murphy G (1997) Activation of progelatinase B (proMMP-9) by active collagenase-3 (MMP-13). Eur. J. Biochem., 248: 369-373.
17. Ashworth JL, Murphy G, Rock MJ, Sherratt MJ, Shapiro SD, Shuttleworth CA, Kielty CM (1999) Fibrillin degradation by matrix metalloproteinases: implications for connective tissue remodelling. Biochem. J., 340 (Pt 1): 171-181.
18. Leeman MF, Curran S, Murray GI (2002) The structure, regulation, and function of human matrix metalloproteinase-13. Crit Rev. Biochem. Mol. Biol., 37: 149-166.
19. Cowell S, Knauper V, Stewart ML, D'Ortho MP, Stanton H, Hembry RM, Lopez-Otin C, Reynolds JJ, Murphy G (1998) Induction of matrix metalloproteinase activation cascades based on membrane-type 1 matrix metalloproteinase: associated activation of gelatinase A, gelatinase B and collagenase 3. Biochem. J., 331 (Pt 2): 453-458.
20. Takaishi H, Kimura T, Dalal S, Okada Y, D'Armiento J (2008) Joint diseases and matrix metalloproteinases: a role for MMP-13. Curr. Pharm. Biotechnol., 9: 47-54.
21. Kosaki N, Takaishi H, Kamekura S, Kimura T, Okada Y, Minqi L, Amizuka N, Chung UI, Nakamura K, Kawaguchi H, Toyama Y, D'Armiento J (2007) Impaired bone fracture healing in matrix metalloproteinase-13 deficient mice. Biochem. Biophys. Res. Commun., 354: 846-851.
22. Zijlstra A, Aimes RT, Zhu D, Regazzoni K, Kupriyanova T, Seandel M, Deryugina EI, Quigley JP (2004) Collagenolysis-dependent angiogenesis mediated by matrix metalloproteinase-13 (collagenase-3). J. Biol. Chem., 279: 27633-27645.
23. Kosaki N, Takaishi H, Kamekura S, Kimura T, Okada Y, Minqi L, Amizuka N, Chung UI, Nakamura K, Kawaguchi H, Toyama Y, D'Armiento J (2007) Impaired bone fracture healing in matrix metalloproteinase-13 deficient mice. Biochem. Biophys. Res. Commun., 354: 846-851.
24. Lederle W, Hartenstein B, Meides A, Kunzelmann H, Werb Z, Angel P, Mueller MM (2009) MMP13 as a stromal mediator in controlling persistent angiogenesis in skin carcinoma. Carcinogenesis.
25. Inada M, Wang Y, Byrne MH, Rahman MU, Miyaura C, Lopez-Otin C, Krane SM (2004) Critical roles for collagenase-3 (Mmp13) in development of growth plate cartilage and in endochondral ossification. Proc. Natl. Acad. Sci. U. S. A, 101: 17192-17197.
26. Jost M, Maillard C, Lecomte J, Lambert V, Tjwa M, Blaise P, Alvarez Gonzalez ML, Bajou K, Blacher S, Motte P, Humblet C, Defresne MP, Thiry M, Frankenne F, Gothot A, Carmeliet P, Rakic JM, Foidart JM, Noel A (2007) Tumoral and choroidal vascularization: differential cellular mechanisms involving plasminogen activator inhibitor type I. Am. J. Pathol., 171: 1369-1380.
27. Lambert V, Munaut C, Noel A, Frankenne F, Bajou K, Gerard R, Carmeliet P, Defresne MP, Foidart JM, Rakic JM (2001) Influence of plasminogen activator inhibitor type 1 on choroidal neovascularization. FASEB J., 15: 1021-1027.

28. Lambert V, Wielockx B, Munaut C, Galopin C, Jost M, Itoh T, Werb Z, Baker A, Libert C, Krell HW, Foidart JM, Noel A, Rakic JM (2003) MMP-2 and MMP-9 synergize in promoting choroidal neovascularization. FASEB J., 17: 2290-2292.
29. Rakic JM, Maillard C, Jost M, Bajou K, Masson V, Devy L, Lambert V, Foidart JM, Noel A (2003) Role of plasminogen activator-plasmin system in tumor angiogenesis. Cell Mol. Life Sci., 60: 463-473.
30. Rakic JM, Lambert V, Devy L, Luttun A, Carmeliet P, Claes C, Nguyen L, Foidart JM, Noel A, Munaut C (2003) Placental growth factor, a member of the VEGF family, contributes to the development of choroidal neovascularization. Invest Ophthalmol. Vis. Sci., 44: 3186-3193.
31. Rakic JM, Lambert V, Munaut C, Bajou K, Peyrollier K, Alvarez-Gonzalez ML, Carmeliet P, Foidart JM, Noel A (2003) Mice without uPA, tPA, or plasminogen genes are resistant to experimental choroidal neovascularization. Invest Ophthalmol. Vis. Sci., 44: 1732-1739.
32. Lambert V, Munaut C, Jost M, Noel A, Werb Z, Foidart JM, Rakic JM (2002) Matrix metalloproteinase-9 contributes to choroidal neovascularization. Am. J. Pathol., 161: 1247-1253.
33. Inada M, Wang Y, Byrne MH, Rahman MU, Miyaura C, Lopez-Otin C, Krane SM (2004) Critical roles for collagenase-3 (Mmp13) in development of growth plate cartilage and in endochondral ossification. Proc. Natl. Acad. Sci. U. S. A, 101: 17192-17197.
34. El Hour M, Moncada-Pazos A, Blacher S, Masset A, Cal S, Berndt S, Detilleux J, Host L, Obaya AJ, Maillard C, Foidart JM, Ectors F, Noel A, Lopez-Otin C (2010) Higher sensitivity of Adamts12-deficient mice to tumor growth and angiogenesis. Oncogene.
35. Peister A, Mellad JA, Larson BL, Hall BM, Gibson LF, Prockop DJ (2004) Adult stem cells from bone marrow (MSCs) isolated from different strains of inbred mice vary in surface epitopes, rates of proliferation, and differentiation potential. Blood, 103: 1662-1668.
36. Rakic JM, Lambert V, Devy L, Luttun A, Carmeliet P, Claes C, Nguyen L, Foidart JM, Noel A, Munaut C (2003) Placental growth factor, a member of the VEGF family, contributes to the development of choroidal neovascularization. Invest Ophthalmol. Vis. Sci., 44: 3186-3193.
37. Jost M, Maillard C, Lecomte J, Lambert V, Tjwa M, Blaise P, Alvarez Gonzalez ML, Bajou K, Blacher S, Motte P, Humblet C, Defresne MP, Thiry M, Frankenne F, Gothot A, Carmeliet P, Rakic JM, Foidart JM, Noel A (2007) Tumoral and choroidal vascularization: differential cellular mechanisms involving plasminogen activator inhibitor type I. Am. J. Pathol., 171: 1369-1380.
38. Lederle W, Hartenstein B, Meides A, Kunzelmann H, Werb Z, Angel P, Mueller MM (2009) MMP13 as a stromal mediator in controlling persistent angiogenesis in skin carcinoma. Carcinogenesis.
39. Zijlstra A, Aimes RT, Zhu D, Regazzoni K, Kupriyanova T, Seandel M, Deryugina EI, Quigley JP (2004) Collagenolysis-dependent angiogenesis mediated by matrix metalloproteinase-13 (collagenase-3). J. Biol. Chem., 279: 27633-27645.
40. Kosaki N, Takaishi H, Kamekura S, Kimura T, Okada Y, Minqi L, Amizuka N, Chung UI, Nakamura K, Kawaguchi H, Toyama Y, D'Armiento J (2007) Impaired bone fracture healing in matrix metalloproteinase-13 deficient mice. Biochem. Biophys. Res. Commun., 354: 846-851.
41. Lederle W, Hartenstein B, Meides A, Kunzelmann H, Werb Z, Angel P, Mueller MM (2009) MMP13 as a stromal mediator in controlling persistent angiogenesis in skin carcinoma. Carcinogenesis.
42. Inada M, Wang Y, Byrne MH, Rahman MU, Miyaura C, Lopez-Otin C, Krane SM (2004) Critical roles for collagenase-3 (Mmp13) in development of growth plate cartilage and in endochondral ossification. Proc. Natl. Acad. Sci. U. S. A, 101: 17192-17197.
43. Knauper V, Will H, Lopez-Otin C, Smith B, Atkinson SJ, Stanton H, Hembry RM, Murphy G (1996) Cellular mechanisms for human procollagenase-3 (MMP-13) activation. Evidence that MT1-MMP (MMP-14) and gelatinase a (MMP-2) are able to generate active enzyme. J. Biol. Chem., 271: 17124-17131.

44. Lambert V, Wielockx B, Munaut C, Galopin C, Jost M, Itoh T, Werb Z, Baker A, Libert C, Krell HW, Foidart JM, Noel A, Rakic JM (2003) MMP-2 and MMP-9 synergize in promoting choroidal neovascularization. FASEB J., 17: 2290-2292.
45. Whitelock JM, Murdoch AD, Iozzo RV, Underwood PA (1996) The degradation of human endothelial cell-derived perlecan and release of bound basic fibroblast growth factor by stromelysin, collagenase, plasmin, and heparanases. J. Biol. Chem., 271: 10079-10086.
46. Lederle W, Hartenstein B, Meides A, Kunzelmann H, Werb Z, Angel P, Mueller MM (2009) MMP13 as a stromal mediator in controlling persistent angiogenesis in skin carcinoma. Carcinogenesis.
47. Jost M, Maillard C, Lecomte J, Lambert V, Tjwa M, Blaise P, Alvarez Gonzalez ML, Bajou K, Blacher S, Motte P, Humblet C, Defresne MP, Thiry M, Frankenne F, Gothot A, Carmeliet P, Rakic JM, Foidart JM, Noel A (2007) Tumoral and choroidal vascularization: differential cellular mechanisms involving plasminogen activator inhibitor type I. Am. J. Pathol., 171: 1369-1380.
48. Asahara T, Masuda H, Takahashi T, Kalka C, Pastore C, Silver M, Kearne M, Magner M, Isner JM (1999) Bone marrow origin of endothelial progenitor cells responsible for postnatal vasculogenesis in physiological and pathological neovascularization. Circ. Res., 85: 221-228.
49. Sengupta N, Caballero S, Mames RN, Butler JM, Scott EW, Grant MB (2003) The role of adult bone marrow-derived stem cells in choroidal neovascularization. Invest Ophthalmol. Vis. Sci., 44: 4908-4913.
50. Jost M, Maillard C, Lecomte J, Lambert V, Tjwa M, Blaise P, Alvarez Gonzalez ML, Bajou K, Blacher S, Motte P, Humblet C, Defresne MP, Thiry M, Frankenne F, Gothot A, Carmeliet P, Rakic JM, Foidart JM, Noel A (2007) Tumoral and choroidal vascularization: differential cellular mechanisms involving plasminogen activator inhibitor type I. Am. J. Pathol., 171: 1369-1380.
51. Sengupta N, Caballero S, Mames RN, Butler JM, Scott EW, Grant MB (2003) The role of adult bone marrow-derived stem cells in choroidal neovascularization. Invest Ophthalmol. Vis. Sci., 44: 4908-4913.
52. Csaky KG, Baffi JZ, Byrnes GA, Wolfe JD, Hilmer SC, Flippin J, Cousins SW (2004) Recruitment of marrow-derived endothelial cells to experimental choroidal neovascularization by local expression of vascular endothelial growth factor. Exp. Eye Res., 78: 1107-1116.
53. Espinosa-Heidmann DG, Caicedo A, Hernandez EP, Csaky KG, Cousins SW (2003) Bone marrow-derived progenitor cells contribute to experimental choroidal neovascularization. Invest Ophthalmol. Vis. Sci., 44: 4914-4919.
54. Tomita M, Yamada H, Adachi Y, Cui Y, Yamada E, Higuchi A, Minamino K, Suzuki Y, Matsumura M, Ikehara S (2004) Choroidal neovascularization is provided by bone marrow cells. Stem Cells, 22: 21-26.
55. Jost M, Maillard C, Lecomte J, Lambert V, Tjwa M, Blaise P, Alvarez Gonzalez ML, Bajou K, Blacher S, Motte P, Humblet C, Defresne MP, Thiry M, Frankenne F, Gothot A, Carmeliet P, Rakic JM, Foidart JM, Noel A (2007) Tumoral and choroidal vascularization: differential cellular mechanisms involving plasminogen activator inhibitor type I. Am. J. Pathol., 171: 1369-1380.
56. Sengupta N, Caballero S, Mames RN, Butler JM, Scott EW, Grant MB (2003) The role of adult bone marrow-derived stem cells in choroidal neovascularization. Invest Ophthalmol. Vis. Sci., 44: 4908-4913.
57. Csaky KG, Baffi JZ, Byrnes GA, Wolfe JD, Hilmer SC, Flippin J, Cousins SW (2004) Recruitment of marrow-derived endothelial cells to experimental choroidal neovascularization by local expression of vascular endothelial growth factor. Exp. Eye Res., 78: 1107-1116.
58. Espinosa-Heidmann DG, Caicedo A, Hernandez EP, Csaky KG, Cousins SW (2003) Bone marrow-derived progenitor cells contribute to experimental choroidal neovascularization. Invest Ophthalmol. Vis. Sci., 44: 4914-4919.
59. Higashiyama R, Inagaki Y, Hong YY, Kushida M, Nakao S, Niioka M, Watanabe T, Okano H, Matsuzaki Y, Shiota G, Okazaki I (2007) Bone marrow-derived cells express matrix metalloproteinases and contribute to regression of liver fibrosis in mice. Hepatology, 45: 213-222.

60. Udagawa T, Birsner AE, Wood M, D'Amato RJ (2007) Chronic suppression of angiogenesis following radiation exposure is independent of hematopoietic reconstitution. Cancer Res., 67: 2040-2045.
61. Jost M, Maillard C, Lecomte J, Lambert V, Tjwa M, Blaise P, Alvarez Gonzalez ML, Bajou K, Blacher S, Motte P, Humblet C, Defresne MP, Thiry M, Frankenne F, Gothot A, Carmeliet P, Rakic JM, Foidart JM, Noel A (2007) Tumoral and choroidal vascularization: differential cellular mechanisms involving plasminogen activator inhibitor type I. Am. J. Pathol., 171: 1369-1380.
62. Takaishi H, Kimura T, Dalal S, Okada Y, D'Armiento J (2008) Joint diseases and matrix metalloproteinases: a role for MMP-13. Curr. Pharm. Biotechnol., 9: 47-54.
63. Nielsen BS, Rank F, Lopez JM, Balbin M, Vizoso F, Lund LR, Dano K, Lopez-Otin C (2001) Collagenase-3 expression in breast myofibroblasts as a molecular marker of transition of ductal carcinoma in situ lesions to invasive ductal carcinomas. Cancer Res., 61: 7091-7100.
64. Zhang B, Cao X, Liu Y, Cao W, Zhang F, Zhang S, Li H, Ning L, Fu L, Niu Y, Niu R, Sun B, Hao X (2008) Tumor-derived matrix metalloproteinase-13 (MMP-13) correlates with poor prognoses of invasive breast cancer. BMC. Cancer, 8: 83.
65. Noel A, Jost M, Lambert V, Lecomte J, Rakic JM (2007) Anti-angiogenic therapy of exudative age-related macular degeneration: current progress and emerging concepts. Trends Mol. Med., 13: 345-352.

Figure 1. *Mmp13* expression is induced during CNV

A. Representative example of MMP13 mRNA expression in surgically extracted choroidal neovascular membranes of patients with exudative AMD (1 to 3; n=3). Intact posterior segments from healthy donors collected maximum 8 hours after death were used as controls (n = 4). 28S rRNA and GAPDH mRNA were used as a control to check for RNA degradation. Samples were harvested from tissue in (M) or out of the macula (O) (4 to 7; n=4).

B and C. RT-PCR analysis of *Mmp13* mRNA expression in experimental CNV induced by laser burn in mice. RNA were extracted from the entire posterior segment prepared at different times (D0 to D14) after laser burn (B). *Mmp13* mRNA expression was analyzed after microdissection of intact choroid (intact choroid), burned choroid of *WT* mice (*WT* lesion) and *Mmp13*$^{-/-}$ mice (*Mmp13*$^{-/-}$ lesion) (C). The graphs illustrate the densitometric quantification of *Mmp13* mRNA expression normalized to *28S* mRNA. ($*$ *: p<0.05; $**$: p<0.01; $***$: p<0.001).

Figure 2. *Mmp13* deficiency impairs CNV formation

A. Confocal observation of neovascularization on flatmounted eyes 14 days after laser burn. Mice were intraveinously injected with FITC-conjugated Dextran before sacrifice. Fluorescent neovessels were visualized on flatmount choroids by confocal microscopy and their areas were quantified by computerized analysis (graph). **B.** Histological analysis of choroidal lesion. Sections of laser-burned eyes resected from *WT* and *Mmp13*$^{-/-}$ mice at day 14 were stained with hematoxylin-eosin. The white bars delineate the total thickness from the bottom of choroid to the top of lesion (b) and the thickness of adjacent normal choroid (c). The neovascular reaction was quantified by determining the b/c ratio (graph). Number of impacts per experiment group: Ni= 36 to 40. Unpaired Student's *t* test was used as statistical analysis to generate *p* value. ($*$ *: p<0.05; $***$: p<0.001)

Figure 3. Angiogenesis and inflammation are reduced in neovascular lesions of Mmp13-deficient mice. Immunostaining was performed on samples from *WT* and *Mmp13*$^{-/-}$ mice.

A,B : MMP13 immunostaining (day 14). PECAM (red) and NG2 (green) (C,E) or αSMA (green) (E,F) double immunostaining (day 14). G,H : Labelling of inflammatory cells using CD11b antibody (day 5). I,J: Staining of neutrophils (day 5). White bars represent 100µm; yellow dotted line delineate the lesion; R: Retina; Ch: Choroid; inserts represent a 2-fold higher magnification of initial pictures.

Figure 4. Bone marrow transplantation restores CNV formation in *Mmp13*-deficient mice

Mice were irradiated (recipient mice) and engrafted with bone marrow (BM) before laser-induced CNV. Quantification of lesion was performed by analysing the size of CNV on choroidal flatmounts (A) and histological sections (B) (b/c ratio as described in Material and Methods and in Fig. 1). Recipient mice and BM engraftment are indicated below each graph. Number of impacts (Ni) per experiment group: Ni=8 to 12. ($*$ *: p<0.05; $**$: p<0.01; $***$: p<0.001)

Figure 5. MSC intraveinous injections partially restore CNV formation in *MMP13*-deficient mice

MSC issued from *WT* mice were injected 4 times into the tail vein of *WT* and *Mmp13*$^{-/-}$ mice. The effects of MSC injection on CNV was observed at day 14 after laser injury. Quantification of lesion areas were performed by computer-assisted image analysis as described in Materials and Methods (see also legend of Figure 1). Number of impacts per experiment group: Ni=13-28. ($*$ *: p<0.05; $**$: p<0.01)

Figure 1

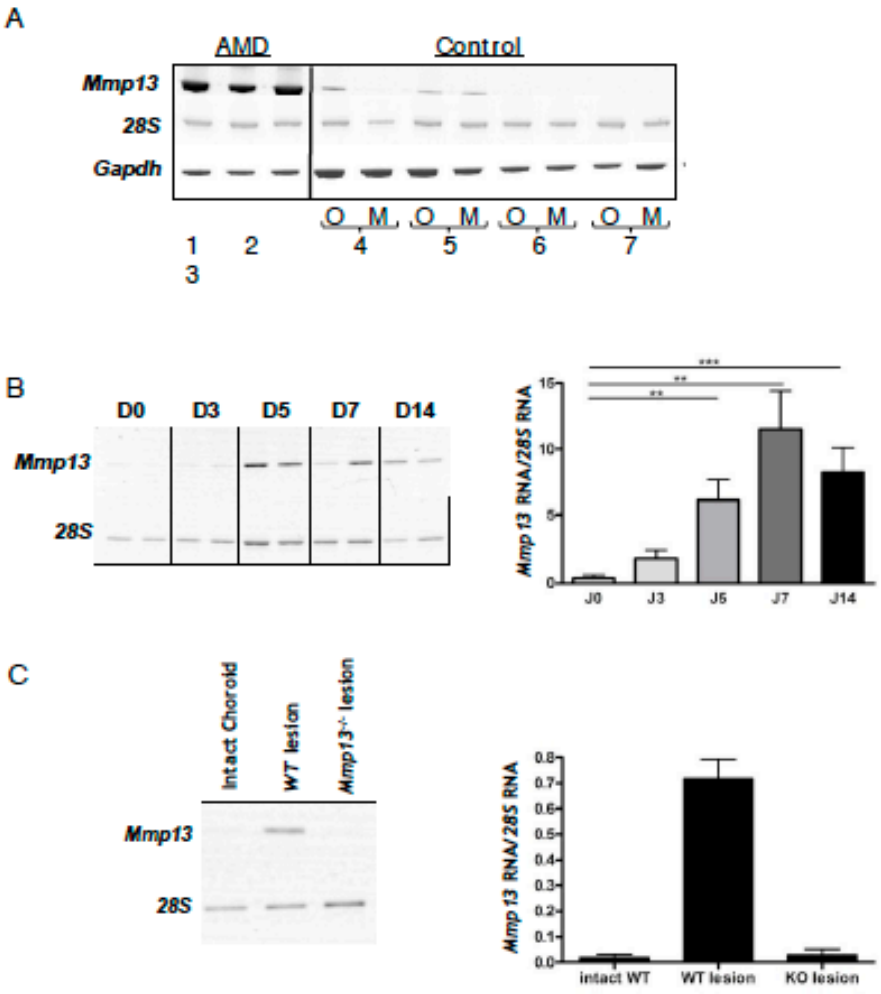
A
AMD
Control
Mmp13
28S
Gapdh
O M O M O M O M
1 2 3 4 5 6 7
B
D0 D3 D5 D7 D14
Mmp13
28S
Mmp 13 RNA/28S RNA
J0 J3 J5 J7 J14
C
Intact Chorold
WT lesion
Mmp13-/- lesion
Mmp13
28S
Mmp 13 RNA/28S RNA
intact WT
WT lesion
KO lesion

Figure 2

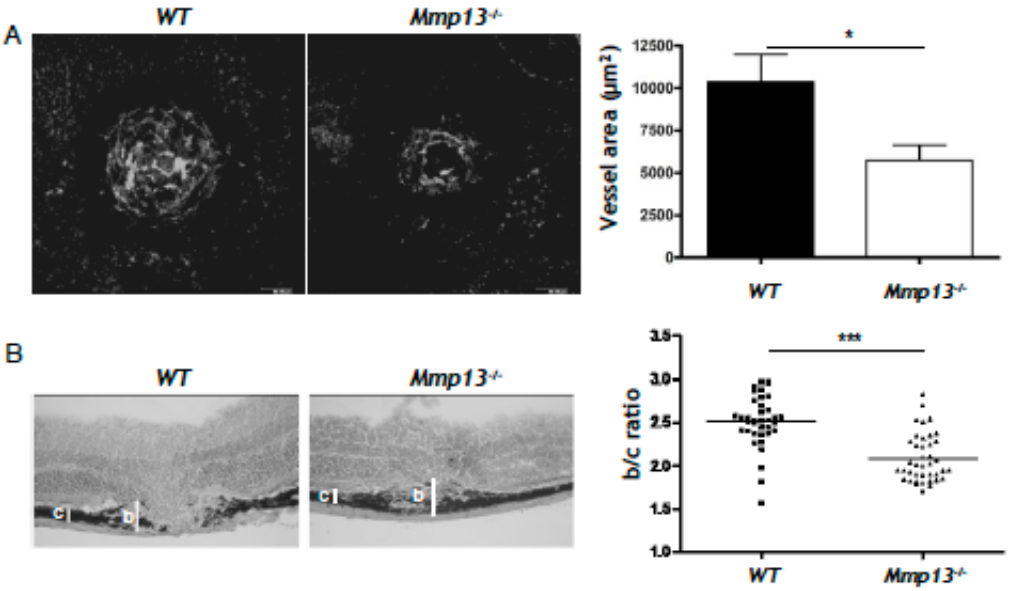
A
WT
Mmp13-/-
Vessel area (µm²)
12500
10000
7500
5000
2500
0
*
WT
Mmp13-/-
B
WT
Mmp13-/-
c
b
c
b
b/c ratio
3.5
3.0
2.5
2.0
1.5
1.0
***
WT
Mmp13-/-

Figure 3

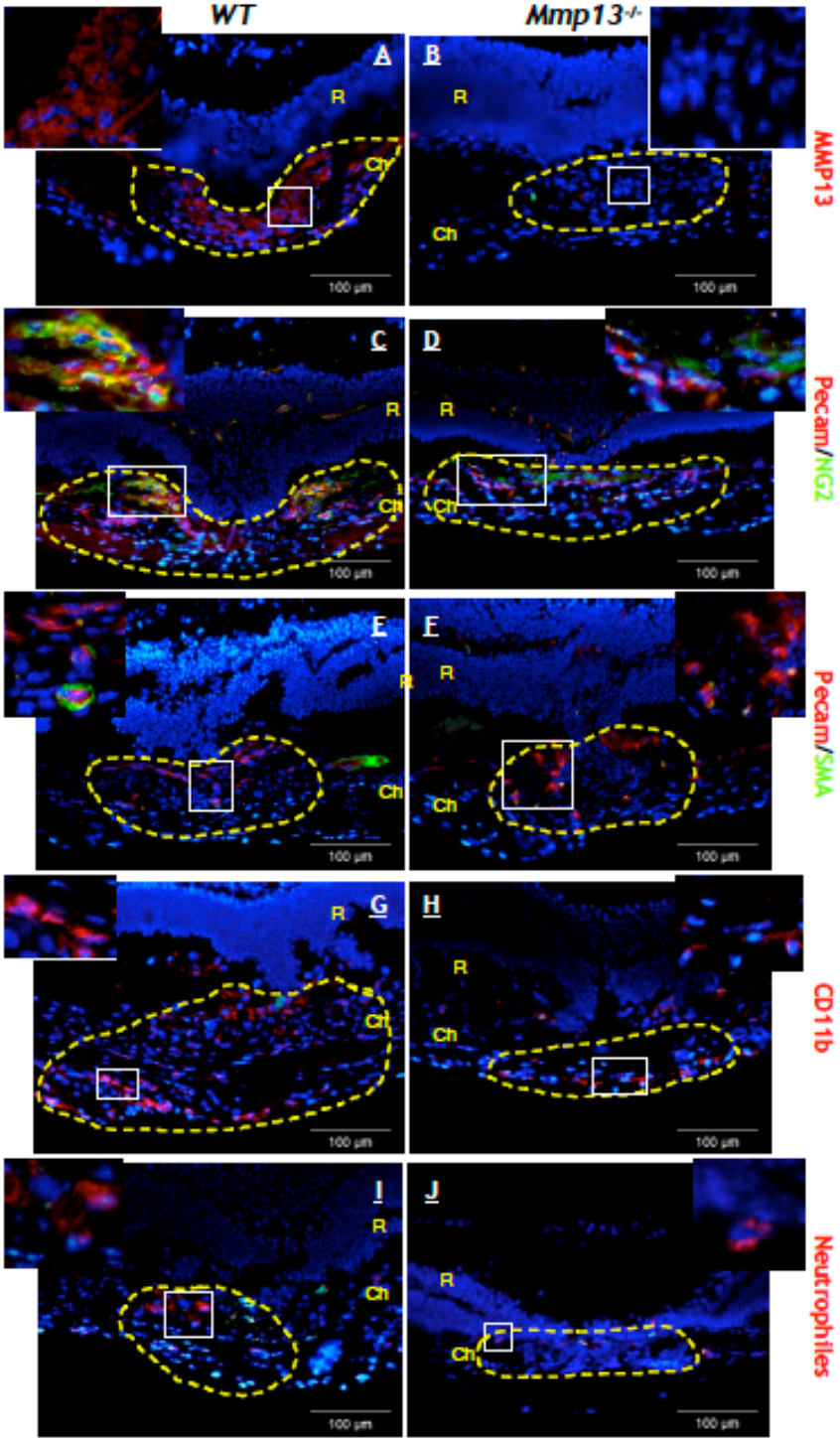
WT
Mmp13-/-
A
B
C
D
E
F
G
H
I
J
R
Ch
100 µm
MMP13
Pecam/NG2
Pecam/SMA
CD11b
Neutrophiles

Figure 4

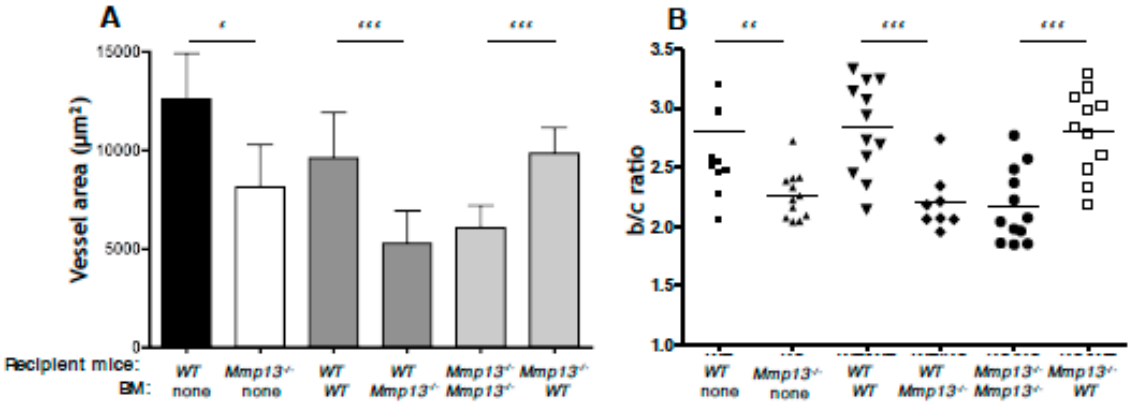
A
B
Vessel area (µm²)
15000
10000
5000
0
b/c ratio
3.5
3.0
2.5
2.0
1.5
1.0
Recipient mice:
BM:
WT
none
Mmp13-/-
none
WT
WT
WT
Mmp13-/-
Mmp13-/-
Mmp13-/-
Mmp13-/-
WT

Figure 5

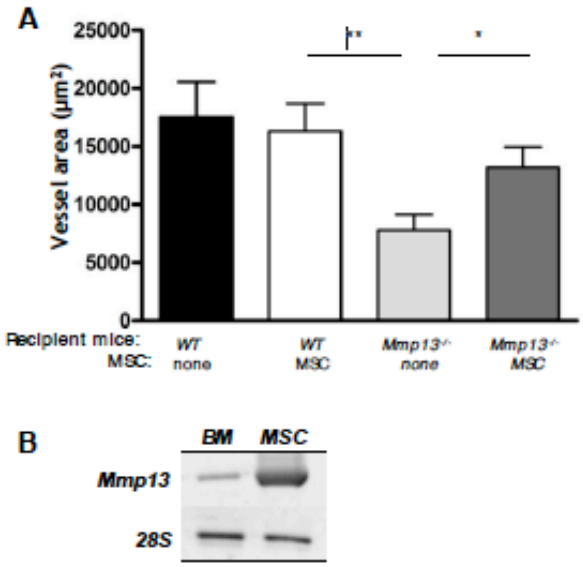
A
25000
20000
15000
10000
5000
0
Vessel area (µm²)
**
*
Recipient mice:
MSC:
WT
none
WT
MSC
Mmp13-/-
none
Mmp13-/-
MSC
B
BM
MSC
Mmp13
28S